

Angiogenesis Inhibition by an Oncolytic Herpes Virus Expressing Interleukin 12

Richard J. Wong,¹ Mei-Ki Chan,² Zhenkun Yu,¹
 Ronald A. Ghossein,³ Ivan Ngai,¹
 Prasad S. Adusumilli,² Brendon M. Stiles,²
 Jatin P. Shah,¹ Bhuvanesh Singh,¹ and
 Yuman Fong²

¹Head and Neck Service, ²Hepatobiliary Service, Department of Surgery, and ³Department of Pathology, Memorial Sloan-Kettering Cancer Center, New York, New York

ABSTRACT

Purpose: Oncolytic herpes simplex viruses (HSVs) may have significant antitumor effects resulting from the direct lysis of cancer cells. HSVs may also be used to express inserted transgenes to exploit additional therapeutic strategies. The ability of an interleukin (IL)-12-expressing HSV to treat squamous cell carcinoma (SCC) by inhibition of tumor angiogenesis is investigated in this study.

Experimental Design: A replication-competent, attenuated, oncolytic HSV carrying the murine IL-12 gene (NV1042), its non-cytokine-carrying analog (NV1023), or saline was used to treat established murine SCC flank tumors by intratumoral injection. The expression of secondary antiangiogenic mediators was measured. Angiogenesis inhibition was assessed by *in vivo* Matrigel plug assays, flank tumor subdermal vascularity, and *in vitro* endothelial cell tubule formation assay.

Results: Intratumoral injections of NV1042 (2×10^7 plaque-forming units) into murine SCC VII flank tumors resulted in smaller tumor volumes as compared with NV1023 or saline. IL-12 and IFN- γ expression in tumors was 440 and 2.2 pg/mg, respectively, at 24 h after NV1042 injection, but both IL-12 and IFN- γ were undetectable (<0.2 pg/mg) after NV1023 or saline injections. Expression of two antiangiogenesis mediators, monokine induced by IFN- γ and IFN-inducible protein 10, was elevated after NV1042 treatment. Matrigel plug assays of NV1042-trans-

fecting SCC VII tumor cells demonstrated significantly decreased hemoglobin content and microvessel density as compared with NV1023 and PBS. Excised murine flank tumors treated with NV1042 had decreased subdermal vascularity as compared with NV1023 and PBS. Both splenocytes and IL-12 expression by NV1042 were required for *in vitro* inhibition of endothelial tubule formation.

Conclusions: IL-12 expression by an oncolytic herpes virus enhances therapy of SCC through antiangiogenic mechanisms. Strategies combining HSV oncolysis with angiogenesis inhibition merit further investigation for potential clinical application.

INTRODUCTION

Replication-competent, attenuated, oncolytic herpes simplex viruses (HSVs) have an ability to infect and lyse a wide variety of malignant tumors. These engineered oncolytic herpes vectors have been shown to have therapeutic effects in treating animal models of brain, breast, prostate, colorectal, and head and neck cancers (1–5). Oncolytic HSVs may be effective when delivered through a variety of routes, including direct intratumoral injection, intracavity [peritoneal (6), bladder (7), and pleural (8)], lymphatic transit (9), intra-arterial perfusion (10), and *i.v.* administration (11).

Several Phase I clinical trials have recently demonstrated encouraging safety data for these attenuated herpes viruses (12–14). Our group has reported the construction and characterization of a series of oncolytic viruses based on the NV1020 (R7020) virus (5, 15, 16). NV1020 was originally designed as a vaccine for HSV-1 and is attenuated by deletions in one copy of the γ_1 34.5 neurovirulence gene, UL56, and the promoter region of UL24 (5, 16). Studies in primates with R7020 demonstrated its relative safety at doses 10,000-fold higher than that of wild-type HSV-1 (17). Furthermore, an ongoing Phase I clinical trial of NV1020 for patients with metastatic colorectal carcinoma has also suggested a favorable safety profile for this oncolytic vector in patients (14).

The predominant mechanism described for the therapeutic effect of these viruses is the direct infection and lysis of malignant cells. However, immune strategies using these oncolytic herpes vectors may also be exploited by designing oncolytic viruses to express cytokine transgenes in an attempt to stimulate a host antitumoral immune response (15, 18, 19). We recently described the construction of NV1042, an attenuated, replication-competent herpes oncolytic vector that carries and expresses an inserted murine interleukin (IL)-12 gene (15). In a murine model of squamous cell carcinoma (SCC), NV1042 displayed significantly enhanced therapeutic effects in comparison with its non-IL-12-expressing analog, NV1023. This effect also conferred immunity to subsequent SCC VII challenge and was abrogated when T-lymphocyte activity was blocked (15).

IL-12 is a cytokine with stimulatory effects on helper T lymphocytes, CTLs, and natural killer cells (20). IL-12 deliv-

Received 1/14/04; revised 2/26/04; accepted 3/4/04.

Grant support: R. J. Wong was supported by a Young Investigator Award from the American Society of Clinical Oncology and a Young Investigator Research Career Development Award from the American Head and Neck Society. Y. Fong was supported in part by NIH Grants RO1CA75416, RO1CA72632, and RO1CA61524 and American Cancer Society Grant MBC-99366.

The costs of publication of this article were defrayed in part by the payment of page charges. This article must therefore be hereby marked *advertisement* in accordance with 18 U.S.C. Section 1734 solely to indicate this fact.

Requests for reprints: Richard J. Wong, Head and Neck Service, C-1069, Memorial Sloan-Kettering Cancer Center, 1275 York Avenue, New York, NY 10021. Phone: (212) 639-7639; Fax: (212) 717-3302; E-mail: wongr@mskcc.org.

ered to established murine tumors may result in significant antitumor effects through the activation of CTLs and natural killer cells (21–22). IL-12 also possesses antiangiogenic effects, which result from the induction of IFN- γ from helper T lymphocytes and the subsequent stimulation of secondary mediators, including monokine induced by IFN- γ (MIG) and IFN-inducible protein 10 (IP-10; Ref. 23). Delivery of IL-12 to malignant tumors by systemic IL-12 administration, plasmid electroporation, adenoviral gene transfer, and IL-12 fusion to an antibody fragment has been shown to result in antiangiogenic effects in animal models (24–27).

The purpose of the present study is to determine whether angiogenesis inhibition may serve as a mechanism to enhance herpes oncolytic viral therapy. Angiogenesis inhibition by a herpes oncolytic vector has not been reported previously. Although IL-12 has been shown to have antiangiogenic effects, IL-12 expression by a herpes oncolytic vector may not necessarily induce effects similar to those of other methods of IL-12 delivery. The local milieu at the site of herpes oncolytic viral delivery is in significant flux, with complex interactions occurring between lysed tumor cells, released progeny viral particles, and recruited immune cells. It is not known whether IL-12-mediated angiogenesis inhibition may be induced in such an environment. The purpose of the present study was to assess the potential antiangiogenic effects of a replication-competent, oncolytic, herpes virus expressing IL-12 (NV1042) in a murine model of SCC.

MATERIALS AND METHODS

Cell Lines. The murine SCC VII cell line is a cutaneous SCC that spontaneously arose from the C3H/HeJ mouse. SCC VII is a poorly immunogenic, rapidly dividing cell line with an estimated doubling time of 18 h (28–30). SCC VII cells were grown *in vitro* in MEM containing 10% FCS, penicillin, and streptomycin under standard cell culture conditions. Human umbilical vein endothelial cells were grown in F12K media with 10% FCS, 1.5 g/liter sodium bicarbonate, 0.1 mg/ml heparin, 0.05 mg/ml endothelial cell growth factor, penicillin, and streptomycin. Murine splenocytes were harvested from C3H/HeJ mice and maintained in RPMI 1640 with nonessential amino acids, penicillin, streptomycin, and 2-mercaptoethanol ($0.5 \text{ cc of } 5.5 \times 10^{-2} \text{ M}$).

Viruses. NV1023 and NV1042 are attenuated, replication-competent, oncolytic herpes viruses whose construction has been described previously (15). NV1023 and NV1042 are derived from NV1020, a selected clone of previously described herpes strain R7020, which was originally designed as a potential vaccine (5, 15, 16). NV1020 contains deletions in UL23/4, UL56, the $\gamma_{134.5}$ neurovirulence gene, and the internal inverted repeat (joint) region. NV1020 also contains an insertion of a HSV-2 fragment and an insertion of the endogenous copy of UL23 (thymidine kinase) into the deleted joint region. NV1023 was constructed by deleting the exogenous copy of thymidine kinase and repairing the UL23/4 locus. NV1042 was constructed by replacing the exogenous copy of thymidine kinase with murine IL-12 under the control of a hybrid α 4-thymidine kinase promoter and by repairing the UL23/4 locus (15). Viruses were provided by MediGene, Inc. (San Diego, CA).

Animals. Animal use was approved by the Memorial Sloan-Kettering (New York, NY) Institutional Animal Care and Use Committee. Approximately 6–8-week-old male C3H/HeJ mice (The Jackson Laboratory, Bar Harbor, ME) were used. Flank tumors were established by s.c. injection of SCC VII cells (5×10^5) in 50 μ l of PBS. Visible tumor nodules were reliably detected in approximately 5 days. Matrigel plugs were established by the s.c. injection of treated SCC VII cells suspended in Matrigel (BD Biosciences, Bedford, MA) into the bilateral ventral groins of mice. Injection of SCC VII cells, virus, or Matrigel into animals was performed under general anesthesia consisting of ketamine (70 μ g) and xylazine (20 μ g) in 100 μ l of sterile water administered by i.p. injection. Animals were sacrificed by CO₂ inhalation.

Oncolytic Viral Therapy of SCC VII Flank Tumors. We sought to determine whether IL-12 expression by NV1042 may confer a therapeutic benefit for relatively large tumors, which are generally less sensitive to purely oncolytic HSV therapy. SCC VII flank tumors were established in mice. When tumors reached a size of approximately 130 mm³ in volume, tumors were measured, and animals were distributed equitably into three groups. Animals ($n = 5$ mice/group) were each treated with a single intratumoral injection of PBS, NV1023 [2×10^7 plaque-forming units (pfu)], or NV1042 (2×10^7 pfu) in 100- μ l volume. Tumor dimensions were measured every 2 days, and volumes were calculated by the formula for the volume of an ellipsoid: volume = $(4/3) \times \pi \times (\text{length}/2) \times (\text{width}/2)^2$.

IL-12 and IFN- γ ELISA. Established s.c. SCC VII flank tumors ($n = 3$ tumors/group) were treated with PBS, NV1023 (2×10^7 pfu), or NV1042 (2×10^7 pfu) in 100- μ l volume by intratumoral injection. Animals were sacrificed at days 1, 3, and 5. Tumor portions were excised, weighed, and homogenized in 1 ml of tissue lysis buffer (T-PER; Pierce Biotechnology, Rockford, IL). IL-12 and IFN- γ levels were determined by ELISA (R&D Systems, Minneapolis, MN) and quantified by spectrophotometry.

MIG and IP-10 Western Blot. Established s.c. SCC VII flank tumors ($n = 3$ tumors/group) were treated with PBS, NV1023 (2×10^7 pfu), or NV1042 (2×10^7 pfu) in 100- μ l volume by intratumoral injection. Animals were sacrificed at day 1, and tumors were excised, weighed, and homogenized in tissue lysis buffer (T-PER; Pierce Biotechnology). Lysed tumor samples underwent electrophoresis on a polyacrylamide gel (Bio-Rad) and were transferred onto a polyvinylidene difluoride membrane. Primary antimouse antibodies for murine IP-10 (CRG-2; R&D Systems), MIG (R&D Systems), and actin (Santa Cruz Biotechnology) were used. An anti-IgG secondary antibody conjugated to horseradish peroxidase (Santa Cruz Biotechnology) was used to visualize IP-10 and MIG with chemiluminescence.

Matrigel Plug Hemoglobin (Hb) Assay and Microvessel Density. SCC VII cells (5×10^5 cells) were infected with PBS, NV1023, or NV1042 (5×10^5 viral pfu) in an Eppendorf tube for 30 min at 37°C. Treated cells were then mixed with 400 μ l of cold Matrigel and injected with an insulin syringe into the ventral groins of C3H/HeJ mice. Twelve days later, animals were sacrificed, and Matrigel plugs were excised.

For the Hb assays, excised plugs ($n = 6$ plugs/group) were placed in 300 μ l of cold PBS at 4°C overnight to liquefy the

Matrigel. Specimens were centrifuged at 14,000 rpm, and the supernatant was collected. Hb content was quantified with Drabkin's reagent kit (Sigma-Aldrich, St. Louis, MO) and spectrophotometry.

For microvessel counting studies, excised plugs ($n = 5$ plugs/group) were fixed in 10% buffered formalin. Matrigel plugs were embedded in paraffin, sectioned on glass slides, and stained with H&E. Slides were reviewed by an experienced pathologist who quantified the number of microvessels per a minimum of 10 high-power fields for each excised plug.

Flank Tumor Subdermal Vascularity. Established s.c. SCC VII flank tumors of varying initial sizes were treated with a single intratumoral injection of saline, NV1023 (2×10^7 pfu), or NV1042 (2×10^7 pfu). Large initial tumors were selected for NV1042 injection, moderate-sized tumors were selected for NV1023 injection, and smaller tumors were selected for saline injection. One week later, animals were sacrificed, and tumors of equitable volume were selected from each group ($n = 3$ tumors/group). Tumors were excised with an adjacent area of dermis and assessed for extent of tumor vascularity along the undersurface of the dermis leading to the tumor. The number of visible subdermal vessels entering the tumor was recorded.

Endothelial Cell Coculture Proliferation and Tubule Formation Assays. To assess the ability of NV1042 to inhibit endothelial cell tubule formation *in vitro*, a coculture experiment was performed *in vitro*, similar to a previously described protocol (31). Murine IL-12 has previously been demonstrated to have activity on human cells (32). Human umbilical vein endothelial cells (2×10^4) were seeded in 6-well plates. SCC VII cells (3×10^4) were added into Anopore membrane inserts (Nunc, Rochester, NY) with 0.02- μm pores, which were placed within the 6-well plates. These inserts allow for coculture of the two cell lines with free exchange of proteins, but no exchange of cells or viral particles. Six h later, PBS, NV1023, or NV1042 (1.5×10^5 pfu) was added to the SCC VII cells. Splenocytes (2×10^6) stimulated with concanavalin A (2 $\mu\text{g}/\text{ml}$) harvested from normal mice were added 24 h later into selected inserts. Cocultures were incubated for 6 days. Human umbilical vein endothelial cell proliferation from each well was calculated by lactate dehydrogenase assay (CytoTox 96 Assay; Promega, Madison, WI). Supernatant from each well (external to the insert) was collected and concentrated in a Centricon tube (YM-3; Millipore, Bedford, MA) with a M_r 3000 cutoff.

Matrigel (300 μl) was plated in 24-well plates overnight and then seeded with human umbilical vein endothelial cells (4×10^4) in fresh media (100 μl) mixed with concentrated supernatant samples (200 μl). Endostatin (20 $\mu\text{g}/\text{ml}$) was added as a negative control, and fresh medium alone was used as a positive control. Experimental groups consisted of different coculture supernatants: NV1023; NV1023+SPC (NV1023 + splenocytes); NV1042; and NV1042+SPC (NV1042 + splenocytes). Wells were examined for endothelial cell tubule formation at 48 h.

RESULTS

Flank Tumor Volumes. Large (approximately 130- mm^3) flank tumors treated with PBS, NV1023, or NV1042 demonstrated limited tumor volume reduction from treatment with the

purely oncolytic NV1023 ($P =$ nonsignificant). In contrast, tumor volumes were significantly decreased after NV1042 treatment ($P < 0.05$) in comparison with PBS-treated tumors (Fig. 1). At day 13 after treatment, the mean volume \pm SE of PBS-treated tumors was $2780 \pm 149 \text{ mm}^3$, in comparison with $1670 \pm 618 \text{ mm}^3$ for NV1023-treated tumors and $690 \pm 185 \text{ mm}^3$ for NV1042-treated tumors. There were no observed toxicities in any animals attributable to viral therapy. There was no evidence of neurotoxicity, mucosal ulcers, poor grooming, or significant weight loss.

IL-12 and IFN- γ ELISA. Established flank tumors treated with a single intratumoral injection of PBS, NV1023, or NV1042 were excised, homogenized, and assayed for IL-12 and IFN- γ by ELISA. At day 1, the level of IL-12 was 440 pg/mg tissue, followed by a rapid decline (Fig. 2). By day 3, the level of IL-12 was 10.4 pg/mg, and by day 5, it was 2.0 pg/mg. In contrast, PBS- and NV1023-treated tumors exhibited undetectable levels of IL-12 (<0.05 pg/mg tissue) at all time points.

IFN- γ levels assessed by ELISA measured 2.2 pg/mg tissue at day 1, 1.1 pg/mg tissue at day 3, and 1.6 pg/mg tissue at day 5 in NV1042-treated tumors (Fig. 3). NV1023-treated tumors had undetectable levels of IFN- γ at days 1 and 3 (<0.2 pg/mg tissue), although at day 5, IFN- γ was slightly elevated at 0.5 pg/mg tissue. Levels of IFN- γ in PBS-treated tumors remained undetectable (<0.2 pg/mg tissue) at all time points.

MIG and IP-10 Western Blot. MIG and IP-10 were both significantly expressed in all three of the flank tumors at 24 h after intratumoral injection of NV1042, and each was highly expressed in two of the three tumors (Fig. 4). NV1023-treated tumors demonstrated lower but detectable levels of MIG and IP-10 expression. None of the saline-treated tumors demonstrated any detectable MIG or IP-10.

Matrigel Plug Hb Assay. Excised Matrigel plugs containing PBS-, NV1023-, or NV1042-treated SCC VII cells were

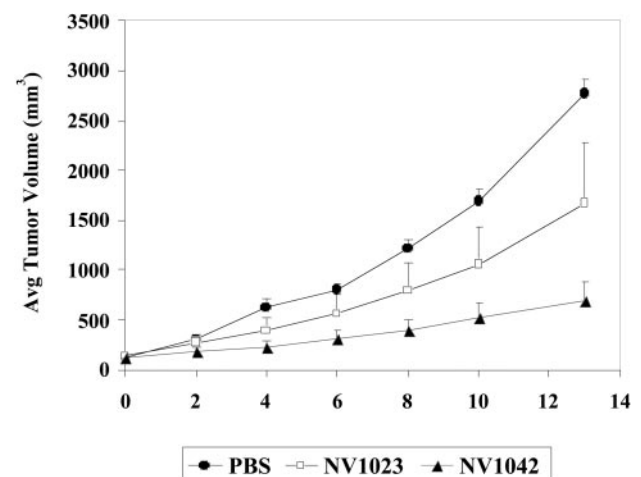


Fig. 1 Large squamous cell carcinoma VII flank tumors were treated with a single intratumoral injection of PBS, NV1023, or NV1042 (2×10^7 plaque-forming units). Treatment with interleukin 12-expressing NV1042 resulted in a significant reduction in tumor volume ($P < 0.05$) in comparison with PBS. In contrast, only a mild benefit was noted with the non-cytokine-expressing NV1023, as compared with PBS ($P =$ nonsignificant).

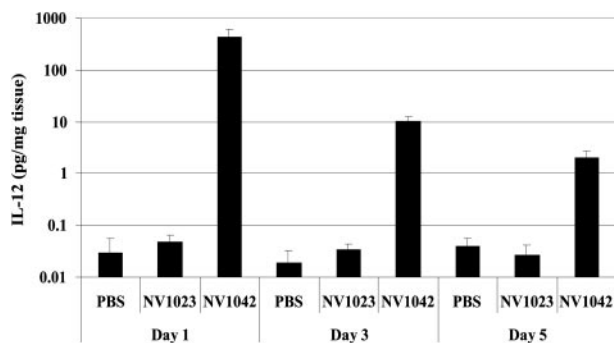


Fig. 2 Interleukin (IL)-12 ELISA was performed on squamous cell carcinoma VII flank tumors treated with a single dose of PBS, NV1023, or NV1042 (2×10^7 plaque-forming units). As assessed by ELISA, there was a high level of IL-12 at 24 h in NV1042-treated tumors, followed by a rapid decline by days 3 and 5. In contrast, IL-12 levels in PBS- and NV1023-treated tumors were undetectable at all time points.

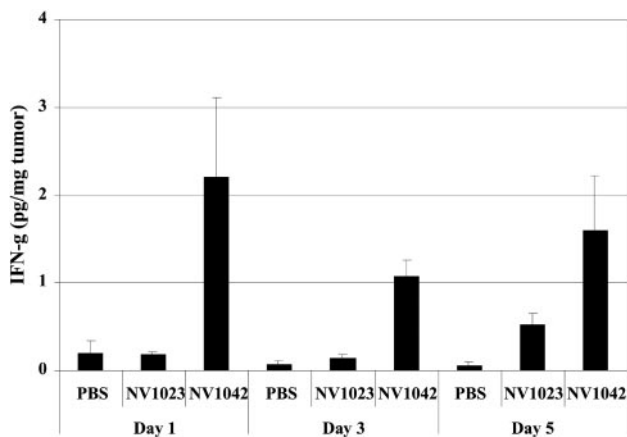


Fig. 3 IFN- γ ELISA was performed on squamous cell carcinoma VII flank tumors treated with a single dose of PBS, NV1023, or NV1042 (2×10^7 plaque-forming units). IFN- γ levels assessed by ELISA demonstrated an initial drop from days 1 to 3, followed by a low-level rise at day 5 in NV1042-treated tumors. Levels were undetectable in NV1023-treated tumors at days 1 and 3, although IFN- γ was slightly elevated at day 5. The delayed, mild elevations of IFN- γ at day 5 for both NV1023- and NV1042-treated tumors may be related to viral oncolytic effects. Levels were undetectable in PBS-treated tumors at all time points.

liquefied and assayed for Hb content. The mean Hb concentration in NV1042-treated Matrigel plugs (15 ± 2 mg Hb/g Matrigel) was significantly lower than NV1023-treated Matrigel plugs (43 ± 7 mg Hb/g Matrigel). The Hb content in the NV1023-treated Matrigel plugs was also found to be significantly lower than that in the saline-treated Matrigel plugs (93 ± 9 mg Hb/g Matrigel; $P < 0.05$, t test for both comparisons; Fig. 5).

Matrigel Plug Endothelial Cell Density. Histology was performed on excised Matrigel plugs, and the average number of microvessels per 10 high-power microscopic fields was quantitated. Matrigel plugs containing saline-treated SCC VII cells demonstrated significant infiltration of the Matrigel with tumor,

with numerous endothelial cell-lined capillaries filled with RBCs. There were an average of 57 ± 5 microvessels/10 high-power microscopic fields in the saline-treated plugs. Matrigel plugs with NV1023-treated SCC VII cells demonstrated moderate SCC VII proliferation with an average of 67 ± 15 microvessels/10 high-power microscopic fields ($P =$ nonsignificant). In contrast, Matrigel plugs with NV1042-treated SCC VII cells displayed sparse, small tumor islands within the Matrigel, with only rare capillaries. NV1042-treated Matrigel plugs had significantly fewer microvessels than NV1023- or PBS-treated Matrigel plugs, with an average of 1.2 ± 0.7 microvessels/10 high-power microscopic fields ($P < 0.05$, t test for both comparisons; Figs. 6 and 7A).

Flank Tumor Subdermal Vascularity. SCC VII flank tumors of varying initial sizes were treated with intratumoral injections of saline, NV1023, or NV1042 (2×10^7 pfu). Seven days later, animals were sacrificed, tumors of similar size from all three groups were selected, and the tumors were excised with the adjacent dermis. Tumors from different groups demonstrated different degrees of feeding tumor vessels along the undersurface of the surrounding dermis. Saline-treated tumors displayed

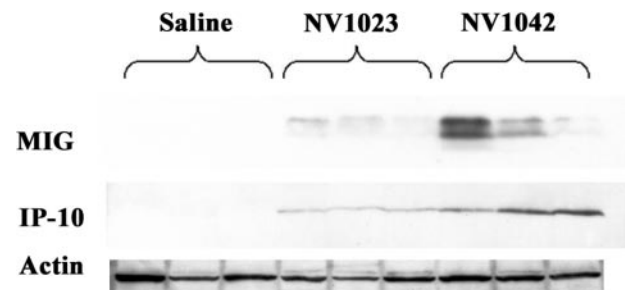


Fig. 4 Monokine induced by IFN- γ (MIG) and IFN-inducible protein 10 (IP-10) were both expressed in flank tumors 1 day after intratumoral injection of NV1042, and each was highly expressed in two of the three tumors. NV1023-treated tumors demonstrated low levels of MIG and IP-10 expression. In contrast, none of the saline-treated tumors demonstrated detectable MIG or IP-10.

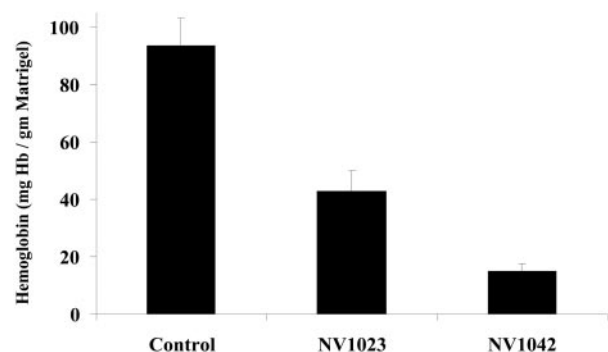


Fig. 5 Excised Matrigel plugs containing PBS-, NV1023-, or NV1042-treated squamous cell carcinoma VII cells were measured by hemoglobin assay. The mean hemoglobin concentration in the NV1042-treated group was significantly lower than that in the NV1023-treated group, which itself was significantly lower than that in the saline-treated group ($P < 0.05$ for both comparisons, t test).

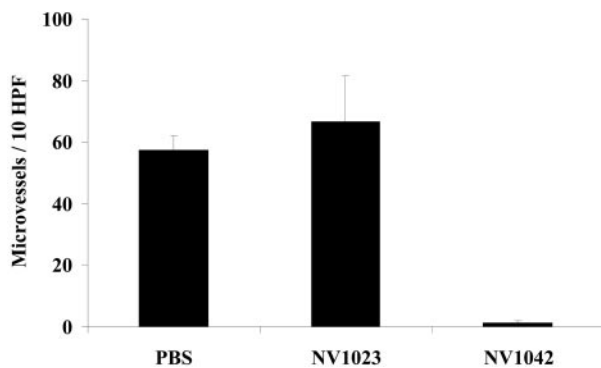


Fig. 6 Histology was performed on excised Matrigel plugs, and the average number of microvessels per 10 high-power microscopic fields was quantitated. Saline-treated Matrigel plugs had a similar microvessel density as saline-treated Matrigel plugs ($P =$ nonsignificant). In contrast, NV1042-treated Matrigel plugs had significantly fewer microvessels than NV1023- or PBS-treated Matrigel plugs, with an average of only 1.2 ± 0.7 microvessels/10 high-power microscopic fields ($P < 0.05$, t test).

multiple large feeding blood vessels (mean, 6.7 ± 1.2). NV1023-treated tumors demonstrated moderate numbers of blood vessels (5.5 ± 1.5), whereas NV1042-treated tumors demonstrated fewer and more narrowed blood vessels (mean, 3.5 ± 0.3 ; Fig. 7B).

Endothelial Cell Coculture Tubule Formation and Proliferation Assay. Endothelial cells cocultured with SCC VII cells treated with PBS, NV1023, or NV1042 showed no significant differences in endothelial cell proliferation rates as measured by lactate dehydrogenase assay (data not shown). Endothelial cells were then grown on Matrigel in coculture supernatants from these groups to observe tubule formation. Endothelial cells grown in complete media showed intact tubule formation, whereas the addition of endostatin inhibited tubule formation. Endothelial cells grown with concentrated supernatant from NV1023- or NV1042-treated SCC VII cells without added splenocytes demonstrated intact tubule formation. Similarly, endothelial cells grown in supernatant from NV1023-treated SCC VII cells with splenocytes also demonstrated intact tubule formation. In contrast, supernatant from NV1042-treated SCC VII cells with added splenocytes led to an inhibition of endothelial cell tubule formation (Fig. 8). This finding suggests that both IL-12 expression by NV1042 and factors released from interacting immune cells are necessary for inhibitory effects on endothelial cell tubule formation.

DISCUSSION

Genetically attenuated, oncolytic HSVs have a remarkable ability to infect and lyse a variety of malignant tumors and are promising cancer therapy agents that have recently reached clinical trials. Furthermore, these DNA viruses allow for relatively large genes of up to 30 kb in size to be inserted into their genome (33). The potential for designing oncolytic herpes viruses to express inserted transgenes opens many possibilities for developing treatment strategies in combination with viral oncolysis. Cytokine gene transfer is one promising strategy. With this approach, an immunostimulatory cytokine carried by the onco-

lytic virus is initially expressed by infected tumor cells. The herpes virus may then replicate and lyse the infected cells, releasing progeny virus to potentially infect other tumor cells. This approach therefore provides (a) cytokine production at the site of the tumor to recruit and stimulate host immune cells; (b) direct lysis of tumor cells; (c) a local environment rich in tumor debris and antigen, to which immune cells have been recruited; and (d) a release of progeny virus to potentially treat other tumor cells. An attractive advantage of this combination strategy is that

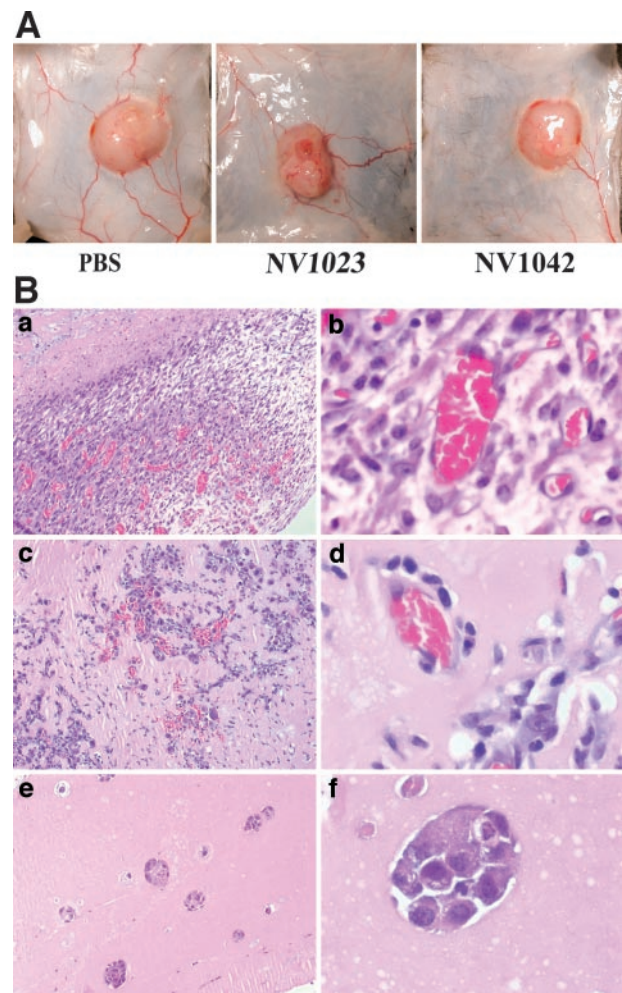


Fig. 7 A, squamous cell carcinoma (SCC) VII flank tumors were treated with intratumoral injections of saline, NV1023, or NV1042 (2×10^7 plaque-forming units). One week later, tumors matched by size were examined for subdermal vascularity. Tumors demonstrated varying degrees of feeding tumor vessels along the undersurface of the surrounding dermis. Saline-treated tumors displayed multiple, large-caliber feeding vessels. NV1023-treated tumors demonstrated fewer feeding vessels, whereas NV1042-treated tumors demonstrated sparse, narrow feeding vessels. B, Matrigel plugs containing saline-treated SCC VII cells demonstrated tumor proliferation and numerous, large-diameter, endothelial cell-lined capillaries filled with RBCs (a, $\times 100$; b, $\times 400$). Matrigel plugs with NV1023-treated SCC VII cells demonstrated numerous, small caliber, endothelial cell-lined capillaries with moderate SCC VII proliferation (c, $\times 100$; d, $\times 400$). In contrast, Matrigel plugs with NV1042-treated SCC VII cells displayed sparse, small tumor islands with only rare capillaries (e, $\times 100$; f, $\times 200$).

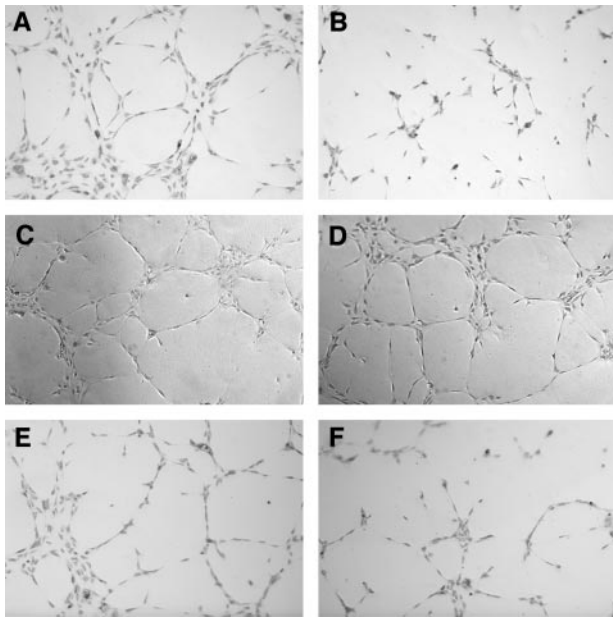


Fig. 8 Endothelial cells were grown on Matrigel to observe tubule formation. Endothelial cells grown in complete media showed intact tubule formation (A), whereas the addition of endostatin inhibited tubule formation (B). Endothelial cells grown with concentrated supernatant from NV1023- or NV1042-treated SCC VII cells without added splenocytes demonstrated intact tubule formation (C and D). Endothelial cells grown in supernatant from NV1023-treated SCC VII cells with splenocytes also demonstrated intact tubule formation (E). However, supernatant from NV1042-treated SCC VII cells with added splenocytes led to an inhibition of endothelial cell tubule formation (F), suggesting that interleukin 12 and immune cells are both necessary for angiogenesis inhibition.

it works through multiple mechanisms of activity. Viral oncolysis is a direct, immediate means of killing tumor cells, whereas cytokine expression elicits a secondary systemic immune response by the host and other potential effects such as inhibition of tumor angiogenesis.

IL-12 is a particularly attractive choice for oncolytic viral gene transfer. IL-12 is normally secreted by antigen-presenting cells such as dendritic cells, monocytes, macrophages, and B lymphocytes. IL-12 stimulates the proliferation and activity of helper T cells, cytotoxic T cells, and natural killer cells, which may have significant antitumoral activity (20). IL-12 immune strategies have recently been explored with oncolytic herpes viruses (15, 19). Our group described the construction of NV1042, a replication-competent, attenuated oncolytic HSV that expresses murine IL-12 under the control of an α 4-thymidine kinase hybrid promoter and also expresses lacZ (15). Flank tumors treated with NV1042 exhibited significantly improved therapeutic effects in comparison with those treated with the purely oncolytic NV023 virus and demonstrated enhanced immunity to subsequent SCC VII challenge. The mechanism of the IL-12-mediated benefit appeared to be related to T-lymphocyte activity and was abrogated in a T-lymphocyte-depleted animal model.

IL-12 has been shown to possess antiangiogenic activity mediated by a stimulation of T-helper lymphocytes and an

induction of IFN- γ . IFN- γ then stimulates the production of MIG (by monocytes) and IP-10 (by a variety of cells including endothelial cells), which have direct antiangiogenic activity (23). The immune and antiangiogenic mechanisms of antitumoral activity by IL-12 are closely linked to each other by the stimulation of T-helper lymphocytes. Our previous finding that blockade of CD4⁺ and CD8⁺ T lymphocytes abrogates the benefit elicited from IL-12 expression is consistent with these findings because loss of T-lymphocyte activity impedes both immune and antiangiogenic effects. IFN- γ induced by IL-12 may also have antiangiogenic effects mediated by natural killer cells (34).

Although IL-12 has previously been shown to inhibit tumor angiogenesis, such an effect after oncolytic HSV delivery has not been described previously. In contrast to previously described methods of IL-12 delivery, the site of oncolytic viral application is a complex mix of infectious viral particles, infected and necrotic tumor cells, cytokines, and a variety of recruited immune cells interacting with one another. It is possible that the interaction of infectious, oncolytic HSV with the cells necessary for angiogenesis inhibition (T-lymphocytes, monocytes, and endothelial cells) might actually impede such an effect. We therefore sought to determine whether IL-12 expression by a replication-competent oncolytic virus may enhance therapy through antiangiogenic mechanisms.

NV1042 treatment of SCC VII flank tumors led to significantly smaller tumor volumes in comparison with control- and NV1023-treated tumors. Intratumoral injections of NV1042 led to a high level of IL-12 expression and the induction of secondary mediators of angiogenesis inhibition including IFN- γ , MIG, and IP-10 (Figs. 3 and 4). Although there was no detectable IL-12 elevation with NV1023 treatment, we noted a low-level elevation in levels of IFN- γ , MIG, and IP-10 after NV1023 treatment. This effect may be related to a purely oncolytic-based induction of T-helper lymphocyte activity. Previous studies have similarly suggested that HSV oncolysis of tumors *in vivo* may serve to induce immune cell activity, even in the absence of cytokine expression (35).

To determine whether there is a direct antiangiogenic effect *in vivo*, we performed Matrigel plug assays. Matrigel plugs containing NV1042-treated SCC VII cells demonstrated significantly lower Hb concentrations and microvessel density in comparison with NV1023-treated and control cells. However, differences in tumor cell proliferation were also observed, raising the question of whether differences in vascularity differences were either (a) truly primary antiangiogenic effects of NV1042 or (b) secondarily related to lower tumor volume resulting from antitumoral immune effects of IL-12. To address this question, s.c. flank tumors were treated with saline, NV1023, or NV1042 and followed for 1 week. Tumors then matched by similar volumes demonstrated fewer subdermal feeding vessels for the NV1042 group, suggesting that differences in vascularity are primarily related to IL-12 and not dependent on tumor volume.

The mechanism for IL-12-mediated angiogenesis inhibition requires the presence of T lymphocytes and monocytes to produce IFN- γ and subsequent mediators such as MIG and IP-10. We therefore performed an *in vitro* coculture experiment

to (a) further demonstrate that angiogenesis inhibition by NV1042 is unrelated to differences in tumor volume and (b) demonstrate the necessity for immune cells in this effect. The ability of endothelial cells on Matrigel to migrate into tubule patterns may be used as an assay for angiogenesis inhibition. Modeled on a previous experiment by Strasly *et al.* (31), we cocultured SCC VII cells infected with NV1042, NV1023, or saline with or without splenocytes. Nonviral media samples from the coculture were concentrated and then assessed for angiogenesis-inhibitory effects on an endothelial cell tubule formation assay. Both IL-12 expression by NV1042 and factors secreted from activated immune cells (splenocytes) were found to be required for inhibition of endothelial cell tubule formation. This finding is consistent with the observation of Strasly *et al.* (31) that IL-12 must interact with immune cells to inhibit endothelial tubule formation (31). IL-12 expression by a replication-competent oncolytic HSV was therefore able to elicit significant antiangiogenic effects.

Interestingly, there was a suggestion that the purely oncolytic NV1023 treatment might result in a very low level of antiangiogenic activity. NV1023 treatment induced a delayed, mild elevation of IFN- γ at day 5 and low but detectable levels of MIG and IP-10 expression. In comparison, there was no detectable IFN- γ , MIG, or IP-10 expression in control tumors treated with PBS. Although there was no difference in microvessel density between PBS- and NV1023-treated Matrigel plugs, Hb levels were significantly decreased in the NV1023 group in comparison with the PBS group. This difference is likely explained by our observation that the vessels in the NV1023 group tended to have a smaller caliber than those from the PBS group and were filled with fewer RBCs. In addition, tumor subdermal vascularity was reduced for NV1023-treated tumors. Viral oncolysis may, in itself, induce antitumoral T-lymphocyte activity (35). This purely oncolytic effect may lead to the low levels of IFN- γ , MIG, and IP-10 generated by NV1023. It is therefore possible that oncolytic viral therapy might induce a low level of angiogenesis inhibition that is significantly potentiated with IL-12 gene transfer.

As engineered, attenuated, oncolytic herpes viruses move closer to clinical application in the treatment of human malignancies, their great potential to exert therapeutic effects through other mechanisms in combination with viral-mediated tumor cell lysis should be explored. The inhibition of tumor angiogenesis is now a major strategic approach being exploited by many new oncology therapies. This study demonstrates that an oncolytic herpes virus may exert significant antiangiogenic effects through IL-12 expression in combination with direct tumor lysis. A potential benefit of NV1042 therapy may ultimately prove to be its ability, as a single agent, to exert antitumor effects through multiple different mechanisms of activity. This multifaceted approach to therapy may be beneficial in both enhancing therapeutic efficacy and potentially reducing the likelihood of tumor resistance. Understanding all of the potential mechanisms of activity by this engineered HSV may provide insights into patient selection for clinical trials. Viral oncolysis, immune stimulation, and antiangiogenesis appear to work well in concert toward achieving effective therapy. This combination

strategy appears promising in preclinical studies and merits further investigation for potential future clinical application.

REFERENCES

1. Mineta T, Rabkin SD, Yazaki T, Hunter WD, Martuza RL. Attenuated multi-mutated herpes simplex virus-1 for the treatment of malignant gliomas. *Nat Med* 1995;1:938–43.
2. Toda M, Rabkin SD, Martuza RL. Treatment of human breast cancer in a brain metastatic model by G207, a replication-competent multimutated herpes simplex virus 1. *Hum Gene Ther* 1998;9:2177–85.
3. Kooby DA, Carew JF, Halterman MW, et al. Oncolytic viral therapy for human colorectal cancer and liver metastases using a multi-mutated herpes simplex virus type-1 (G207). *FASEB J* 1999;13:1325–34.
4. Walker JR, McGeagh KG, Sundaresan P, et al. Local and systemic therapy of human prostate adenocarcinoma with the conditionally replicating herpes simplex virus vector G207. *Hum Gene Ther* 1999;10:2237–43.
5. Wong RJ, Kim SH, Joe JK, et al. Effective treatment of head and neck squamous cell carcinoma by an oncolytic herpes simplex virus. *J Am Coll Surg* 2001;193:12–21.
6. Bennett JJ, Kooby DA, Delman K, et al. Antitumor efficacy of regional oncolytic viral therapy for peritoneally disseminated cancer. *J Mol Med* 2000;78:166–74.
7. Oyama M, Ohigashi T, Hoshi M, et al. Intravesical and intravenous therapy of human bladder cancer by the herpes vector G207. *Hum Gene Ther* 2000;11:1683–93.
8. Ebright MI, Zager JS, Malhotra S, et al. Replication-competent herpes virus NV1020 as direct treatment of pleural cancer in a rat model. *J Thorac Cardiovasc Surg* 2002;124:123–9.
9. Wong RJ, Joe JK, Kim SH, et al. Oncolytic herpesvirus effectively treats murine squamous cell carcinoma and spreads by natural lymphatics to treat sites of lymphatic metastases. *Hum Gene Ther* 2002;13:1213–23.
10. Carew JF, Kooby DA, Halterman MW, Federoff HJ, Fong Y. Selective infection and cytolysis of human head and neck squamous cell carcinoma with sparing of normal mucosa by a cytotoxic herpes simplex virus type 1 (G207). *Hum Gene Ther* 1999;10:1599–606.
11. Wong RJ, Chan M, Yu Z, et al. Effective intravenous therapy of murine pulmonary metastases with an oncolytic herpes virus expressing IL-12. *Clin Cancer Res* 2004;10:251–9.
12. Markert JM, Medlock MD, Rabkin SD, et al. Conditionally replicating herpes simplex virus mutant G207 for the treatment of malignant glioma: results of a Phase I trial. *Gene Ther* 2000;7:867–74.
13. Rampling R, Cruickshank G, Papanastassiou V, et al. Toxicity evaluation of replication-competent herpes simplex virus (ICP 34.5 null mutant 1716) in patients with recurrent malignant glioma. *Gene Ther* 2000;7:859–66.
14. Fong Y, Kemeny N, Jarnagin W, et al. Phase I study of a replication-competent herpes simplex oncolytic virus for treatment of hepatic colorectal metastases. *Proc Am Soc Clin Oncol* 2002;21:8a.
15. Wong RJ, Patel SG, Kim SH, et al. Cytokine gene transfer enhances herpes oncolytic therapy in murine squamous cell carcinoma. *Hum Gene Ther* 2001;12:253–65.
16. Meignier B, Longnecker R, Roizman B. In vivo behavior of genetically engineered herpes simplex viruses R7017 and R7020: construction and evaluation in rodents. *J Infect Dis* 1988;158:602–14.
17. Meignier B, Martin B, Whitley RJ, Roizman B. In vivo behavior of genetically engineered herpes simplex viruses R7017 and R7020. II. Studies in immunocompetent and immunosuppressed owl monkeys (*aotus trivirgatus*). *J Infect Dis* 1990;162:313–21.
18. Andreasky S, He B, van Cott J, et al. Treatment of intracranial gliomas in immunocompetent mice using herpes simplex viruses that express murine interleukins. *Gene Ther* 1998;5:121–30.
19. Parker JN, Gillespie GY, Love CE, et al. Engineered herpes simplex virus expressing IL-12 in the treatment of experimental murine brain tumors. *Proc Natl Acad Sci USA* 2000;97:2208–13.

20. Portielje JE, Gratama JW, van Ojik HH, Stoter G, Kruit WH. IL-12: a promising adjuvant for cancer vaccination. *Cancer Immunol Immunother* 2003;52:133–44.
21. Brunda MJ, Luistro L, Warriar RR, et al. Antitumor and antimetastatic activity of interleukin-12 against murine tumors. *J Exp Med* 178:1223–30.
22. Bramson JL, Hitt M, Addison CL, et al. Direct intratumoral injection of an adenovirus expressing interleukin-12 induces regression and long-lasting immunity that is associated with highly localized expression of interleukin-12. *Hum Gene Ther* 1996;7:1995–2002.
23. Sgadari C, Angiolillo AL, Tosato G. Inhibition of angiogenesis by interleukin-12 is mediated by the interferon-inducible protein 10. *Blood* 1996;7:3877–82.
24. Voest EE, Kenyon BM, O'Reilly MS, et al. Inhibition of angiogenesis in vivo by interleukin 12. *J Natl Cancer Inst (Bethesda)* 1995;87:581–6.
25. Lucas ML, Heller L, Coppola D, Heller R. IL-12 plasmid delivery by in vivo electroporation for the successful treatment of established subcutaneous B16.F10 melanoma. *Mol Ther* 2002;5:668–75.
26. Palmer K, Hitt M, Emtage PC, Gyorffy S, Gauldie J. Combined CXC chemokine and interleukin-12 gene transfer enhances antitumor immunity. *Gene Ther* 2001;8:282–90.
27. Halin C, Rondini S, Nilsson F, et al. Enhancement of the antitumor activity of interleukin-12 by targeted delivery to neovasculature. *Nat Biotechnol* 2002;20:264–9.
28. Fu KK, Rayner PA, Lam KN. Modification of the effects of continuous low-dose radiation by concurrent chemotherapy infusion. *Int J Radiat Oncol Biol Phys* 1984;10:1473–8.
29. O'Malley BW, Cope KA, Johnson CS, Schwartz MR. A new immunocompetent murine model for oral cancer. *Arch Otolaryngol Head Neck Surg* 1997;123:20–4.
30. Khurana D, Martin EA, Kasperbauer JL, et al. Characterization of a spontaneously arising murine squamous cell carcinoma (SCC VII) as a prerequisite for head and neck cancer immunotherapy. *Head Neck* 2001;23:899–906.
31. Strasly M, Cavallo F, Geuna M, et al. IL-12 inhibition of endothelial cell functions and angiogenesis depends on lymphocyte-endothelial cell cross-talk. *J Immunol* 2001;166:3890–9.
32. Schoenhaut DS, Chua AO, Wolitzky AG, et al. Cloning and expression of murine IL-12. *J Immunol* 1992;148:3433–40.
33. Martuza RL. Conditionally replicating herpes vectors for cancer therapy. *J Clin Investig* 2000;105:841–6.
34. Yao L, Sgadari C, Furuke K, et al. Contribution of natural killer cells to inhibition of angiogenesis by interleukin-12. *Blood* 1999;93:1612–21.
35. Todo T, Rabkin SD, Sundaresan P, et al. Systemic antitumor immunity in experimental brain tumor therapy using a multmutated, replication-competent herpes simplex virus. *Hum Gene Ther* 1999;10:2741–55.